Eur. Phys. J. D **32**, 95–111 (2005)
DOI: 10.1140/epjd/e2004-00195-x

THE EUROPEAN PHYSICAL JOURNAL D

Control of amplification without population inversion in H_2 and Li_2 molecules: three level Ladder, V and Λ systems

R.K. Das[1], S. Sanyal[2,a], and K.R. Dastidar[1,b]

[1] Department of Spectroscopy, Indian Association for the Cultivation of Science, Kolkata 700032, India
[2] Jangipur College, Jangipur, West Bengal, India

Received 12 June 2002 / Received in final form 13 July 2004
Published online 4 January 2005 –

Abstract. We have studied (ab-initio) the feasibility of Amplification Without Population Inversion (AWPI) both numerically and analytically, in H_2 and Li_2 molecules for three different three level schemes e.g. (i) Ladder, (ii) V and (iii) Λ. We have shown that the shape of the gain profile (gain as a function of the detuning from upper lasing level) and its magnitude are different for these three transition schemes. We have also shown that the strength of AWPI and its variation with detuning can be controlled by choosing different vibrational levels of the molecule as the upper and lower levels for amplification. Thus AWPI can be obtained in a wide range of frequencies considering transitions between different vibrational levels within the same set of electronic states, in contrast to that in atoms. For three level ladder system, time evolution of gain profile shows that for resonant transitions AWPI can be obtained only for short time duration. It has been shown that AWPI is also feasible in presence of Doppler broadening (which is orders of magnitude greater than the spontaneous decay width in H_2 and Li_2 molecules) if the coherent coupling strength is increased by orders of magnitude.

PACS. 42.50.Gy Effects of atomic coherence on propagation, absorption, and amplification of light; electromagnetically induced transparency and absorption – 42.50.Hz Strong-field excitation of optical transitions in quantum systems; multiphoton processes; dynamic Stark shift

1 Introduction

During the last decade considerable interests in the field of light amplification without population inversion (AWPI) and lasing without population inversion (LWPI) have been studied both theoretically [1–4] and experimentally [5]. Some experimental findings in AWPI of atoms (Na and Rb) are in good agreement with the theoretical calculations [5] (see last two references in [5]). These investigations on AWPI/LWPI have been carried out due to its potentiality for extending the laser sources in the spectral regions in which the population inversion is difficult to achieve, e.g. in UV or VUV spectral region, where lasing occurs in general from highly excited Rydberg/Autoionizing state. Moreover, inversionless lasing gives rise to narrower linewidth (compared to conventional lasers) and amplitude squeezing [6].

The key mechanism underlying this type of lasing is that the absorption becomes minimum or equal to zero due to some destructive interference between different absorption channels, keeping the emission intact. Hence, a small population in the upper lasing level can give rise to light amplification. To minimize the absorption, atomic coherence is set either by (i) some external coherent field [1] or (ii) a system is chosen where atomic coherence is inherent in the medium, (e.g. coherence between autoionizing (AI) states and the continuum embracing the AI states and giving rise to Fano interference) or (iii) the presence of two-photon coherence in chaotic/diffused radiation field [2–4]. To obtain LWPI in absence of any coherent field, in general a multilevel system is chosen of which one or two levels are autoionizing states. In this system the absorption channels to the autoionizing state and the continuum (embracing the autoionizing state) interfere destructively giving rise to minimum absorption, whereas the emission from the upper lasing level remains intact. In our previous calculations we have studied [3] using resolvent operator technique, different interesting features for LWPI in model systems as well as in H_2 molecules (ab-initio calculations) involving autoionizing states. In this case strong coherent field to invoke the atomic coherence is not necessary. The most remarkable feature is that to get lasing from an excited AI state, one has to pump the lower autoionizing state only. This is possible due to the inherent coherence between two AI states caused by configuration interaction coupling via common continuum. We have also shown that the process of LWPI

[a] e-mail: susmitasanyal@yahoo.co.in
[b] e-mail: spkrd@mahendra.iacs.res.in

is affected by the presence of different absorption channels via the near resonant rovibrational levels in H_2 molecules. There is another way of getting LWPI in absence of any coherent field, is to invoke two-photon coherence in presence of chaotic field or diffused radiation field in a three level ladder system [4].

For the LWPI in presence of strong coherent field, the atomic coherence is invoked by coupling at least two levels of the system by the strong coherent field. In this process, one of the strongly coupled states is either the lower lasing level or the upper lasing level. A probe field couples two lasing levels and it is used for registering the LWPI. Different type of schemes [1] (e.g. Ladder, Λ, V etc.) have been proposed in three and four level model systems and have been shown that lasing without population inversion can be obtained for different set of parameters. The physical phenomena involved in case of absorption and emission in V and Λ system and the effect of atomic coherence on these processes have been analyzed by dressed state approach [7]. In a recent study on superfluorescence without population inversion in a three level V system it has been shown that in the pulsed regime an initial Raman Inversion is required for superfluorescence to be possible [8]. It has been shown that in case of Ladder (three level) system inversionless lasing with self generated driving field can be obtained on a fast-decaying transition [8]. The effect of strong coupling of a cavity mode with the intermediate state of a three level Ladder system has also been studied [9]. Amplification on dark transitions in a three level V-system has been studied [10] to understand the physical phenomena involved in these processes. In real systems (e.g. atoms and molecules) most of the calculations have been done using different schemes for the realisation of AWPI in atomic systems [5,11,12]. It has been shown in polyatomic molecule the microwave induced transparency [12] is more efficient than electromagnetically induced transparency in atoms. Role of inhomogeneous broadening on coherent population transfer in polar molecule [15] and on the inversionless lasing in homonuclear diatomic molecule [14] has also been studied.

In this paper we have studied AWPI in molecules (H_2 and Li_2) considering Ladder, V and Λ type transitions involving three vibrational levels of the system and it has been shown that the coherence required for the AWPI can be achieved. Unlike atoms, molecules have extra degrees of freedom such as rotational and vibrational motion which may affect the AWPI processes in different ways. Therefore it is interesting to study the dependence of AWPI on the choice of rovibrational levels of the molecules, involved in the transitions. The evolution of gain (transient and steady state) [13] in three level system has been studied previously. In this work we have studied the evolution of gain profile with time as well as the evolution of populations and coherences in the Doppler broadened three level system (in H_2 and Li_2 molecules). To our knowledge this type of comprehensive ab-initio study in molecules has not been done before. Moreover, in the present work, we have shown the conditions under which AWPI in the VUV/UV and red/infrared spectral range can be obtained in H_2 and Li_2 molecules respectively by considering Doppler Broadening of the molecular levels and this may be tested in the laboratory. In a recent study on Na_2 molecule it has been shown that AWPI is feasible although these molecules have large Doppler width [14]. We have shown that although the Doppler width in H_2 molecules is greater than that in Na_2 molecule, AWPI is feasible in presence of strong coherent coupling. In the study of coherent population transfer, it has been shown [15] that in the presence of Doppler broadening the absorption of probe is enhanced when the Rabi frequency is smaller than the Doppler width. On the study of enhancement of refractive index in phaseonium, it has been shown that for the Doppler width which is one order of magnitude greater than the spontaneous decay width refractive index is damped to be negligible [18]. We have shown here although the AWPI is reduced by orders of magnitude in presence of Doppler width which is several orders of magnitude greater than the spontaneous width one can get AWPI by increasing the intensity of coherent radiation field and also by increasing the gas density to a value for which the collisional width is orders of magnitude less than the Doppler width (see Results and discussion).

In general AWPI is studied in atoms by considering three, four or multilevel schemes, where two closely spaced upper or lower levels are chosen to be hyperfine levels (the spacing between these levels is around 1 GHz depending on the specific atoms). In this work we have shown that for AWPI in molecules one can also choose two rovibrational levels as two upper levels in three level V-system and two lower levels in three level Λ system. Although the spacing between vibrational levels are at least one order of magnitude greater than that between rotational levels and several orders of magnitude greater than the hyperfine splitting (e.g. in the ground state of H_2 molecule vibrational spacing, rotational spacing and hyperfine splitting are of the order of 65842.5 GHz [16], 6584.25 GHz and of the order of 1 MHz [17] respectively), the coherence can be maintained between two vibrational levels, making the AWPI feasible. Moreover the options for choosing different three level systems in molecules by considering transitions between different rovibrational levels are numerous. Hence within a set of two or three electronic states one can consider transitions between several rovibrational levels to get AWPI in a wide range of frequencies which is not possible in atoms. In case of atoms since the hyperfine levels are very close to each other lasers used for probe and strong field should have bandwidth less than this spacing (less than 10^{-3} cm^{-1}) for singling out the individual states. In case of molecules since the vibrational levels are widely spaced this restriction is not required as long as coherence is maintained. It is to be noted that the Doppler width for the diatomic molecules e.g. that in H_2 molecules is of the order of 23.6 GHz, which is orders of magnitude smaller than the rovibrational spacing but several orders of magnitude greater than the hyperfine splitting and is one order of magnitude greater than the total spontaneous decay width of excited levels ($1 \rightarrow 2$ GHz) [16]. Collisional width at room temperature will be 10 MHz when

the atomic/molecular pressure is kept at 1 Torr [18] which is three orders of magnitude less than the Doppler width. Similar study on Coherent Population Transfer in polar molecule has been done considering transitions between different vibrational levels [15].

It is well-known that in case of H_2 molecules, the para molecules (with nuclear spin $I = 0$) will occupy the states with even total angular momentum quantum number ($j = 0$, 2, 4 etc.) and the ortho molecules (with $I = 1$) will occupy the states with odd angular momentum quantum numbers. By using molecular jet one can get most of the populations in $j = 0$ and 1 levels. But one can selectively excite $v = 0$, $j = 0$ level of ground state by choosing the transition frequency appropriately (e.g. energy difference between $v = 0$, $j = 0$ level of ground state of H_2 molecule and $v = 0, j = 1$ level of $B^1\Sigma_u$ state is 90316 cm^{-1}). A simple calculation can show that if the $v = 0$, $j = 1$ level of the ground state is excited by a photon of this energy, it will reach very close to the $v = 0, j = 3$ level of $B^1\Sigma_u$ state (this transition is forbidden) and it will be detuned from the $j = 2$ level by approximately 109.7 cm^{-1}. Therefore the probability for detuned transition from $j = 1$ level of the ground state is much weaker than the resonant transition from $j = 0$ level. Since here the transition from $j = 0$ level of the ground state has been considered, only the $m_j = 0$ level of the excited $j = 1$ level will be populated due to $\Delta m_j = 0$ selection rule (we have considered linearly polarized light). There will be no population distribution among other m_j levels for $\Sigma - \Sigma$ transitions. However for Ladder transition scheme in Li_2 molecule, transitions to three m_j levels in strong $\Sigma - \Pi$ coupling have been taken into account.

In this calculation we have considered three level closed system. But in practice other rovibrational levels of the molecule will take part in the process in the following ways: (1) the excited molecule may spontaneously decay into different rovibrational levels of the allowed lower electronic states and (2) once these levels get populated due to spontaneous decay, there is a possibility that these levels will be further excited by the laser photons taking part in this process.

(1) To include the effect of spontaneous decay to different vibrational levels one will have to consider total spontaneous decay width in place of partial decay width considered in this calculation. But it has been mentioned in the last paragraph that the total spontaneous decay width in H_2 molecule is one order of magnitude less than the Doppler width. We have shown that to get AWPI in presence of large Doppler width one will have to increase the intensity of coherent field so that the ac Stark splitting of levels are greater than the decay width. The incoherent pumping rate should also be increased so that a small fraction of the molecules is excited in the upper lasing level (see Results and discussion). Therefore if we add this total spontaneous width with the Doppler width one will have to slightly increase the intensity of the strong field and the incoherent pumping rate but the results will remain the same qualitatively and almost the same quantitatively as those shown by taking into account of Doppler broadening. It has been shown that in presence of inhomogeneous broadening, effect of homogeneous broadening will be negligible [19].

(2) Now let us consider the effect of further transitions from other rovibrational levels which will be populated due to spontaneous decay from the excited levels, on the amplification process. Let us choose three level V-system in H_2 molecule where the strong field couples the $v = 0$ levels of ground $X^1\Sigma_g$ state and the first excited $B^1\Sigma_u$ state and the probe and pump field act between $v = 0 \rightarrow v_1 = 1$ levels of these two electronic states. The frequencies for these two transitions are 2.70375×10^{15} Hz (photon energy = 90125.214 cm^{-1}) and 2.74334×10^{15} Hz (photon energy = 91444.917 cm^{-1}) respectively. It is well-known that under normal condition the population in $v = 0$ level of the ground state of a molecule is maximum and it decays exponentially with the increase in vibrational quantum number. The higher vibrational levels of the ground state will be populated due to spontaneous decay from these excited levels ($v_1 = 0$ and 1 levels of $B^1\Sigma_u$ state). But in the large time limit these molecules will decay to ground state due to collisional and vibrational relaxation. Within the life time of an excited vibrational level say $v = 1$ level of $X^1\Sigma_g$ state (which is closest to $v = 0$ level), the fraction of the molecules lying in this level may be further excited by the probe and strong fields to higher vibrational levels of $B^1\Sigma_u$ state e.g. strong field will excite the molecule in between $v_1 = 3$ and 4 levels and probe field will excite the molecule in between $v_1 = 4$ and 5 levels and the amplification process will be repeated. But since this will be a second order process and since the frequencies are far away from the exact resonance from these levels, effect of this second order process will be orders of magnitude less than the first order process (i.e. the initial excitation from the $v = 0$ level of the ground state). The total spontaneous decay widths of $v_1 = 3$, 4 and 5 levels of $B^1\Sigma_u$ state are 1.536, 1.448 and 1.349 GHz respectively whereas the detunings of the strong coherent field from $v_1 = 3$ and 4 levels are 9419 GHz and 26973 GHz respectively and those for the probe and pump field from $v_1 = 4$ and 5 levels are 12594 and 22806 GHz respectively. Similarly one may consider further transitions from higher vibrational levels i.e. v greater than 1 of $X^1\Sigma_g$ state but the energy consideration will show that these transitions will be much detuned from different excited vibrational levels (i.e. v_1 greater than 3) of $B^1\Sigma_u$ state. Furthermore the Franck-Condon overlap with higher vibrational levels will decrease with the increase in vibrational quantum number. Hence the transition strengths will be much weaker i.e. will be less by two to three orders of magnitude. Moreover, since these transitions will occur from excited vibrational levels only a small fraction of the molecules will take part in this second order process. Therefore the probability for further transitions from different vibrational levels of $X^1\Sigma_g$ state can be ignored. This is due to the fact that the rovibrational spacing in molecules are orders of magnitude greater than the spontaneous decay width of these levels. For V-system it is found that the maximum gain is obtained for the probe frequency detuned from

the exact resonance. The detuning for the maximum gain with Doppler broadening is of the order of 1316.85 GHz which is one order of magnitude less than those for the transitions from the excited vibrational level $v = 1$ in the ground state (as mentioned above). Therefore at the maximum gain although the probe frequency is detuned from the exact resonance, the effect of further transitions from other vibrational levels can be neglected. In case of Ladder scheme, the loss due to multiphoton ionization from the top most state may affect [20] the AWPI process. But in the present case multiphoton ionization will be a third order process in H_2 molecule for Ladder scheme. For V and Λ transition schemes molecules will be excited to the very high energy ionization continuum from the $B^1\Sigma_u$ state by the strong field VUV photon. Hence the probability for bound-continuum transition (high above the ionization threshold) will be much less than the bound-bound transition.

A simple calculation considering energy spacing between different rovibrational levels in Li_2 molecule (of the order of 6584 GHz in $A^1\Sigma_u$ state and 10534 GHz in $X^1\Sigma_g$ state), its hyperfine splitting [21] (of the order of 1 MHz), total spontaneous decay width (77 MHz from $v = 0$ level of $A^1\Sigma_u$ state) and the Doppler width at room temperature (of the order of 1.5 GHz), it can be shown that the conclusions drawn above for the H_2 molecule on the effect of decay to other rovibrational levels and on the possibility of further transitions from these excited rovibrational levels, will be the same for Li_2 molecule. We have discussed above the case of three level V-system in H_2 and Li_2 molecules. Due to lack of space we have not discussed here other two transition schemes. But from the data given in this paper (see Results and discussion and the figure captions) and the energy values and spontaneous decay widths given in the literature [16,22], it can be shown that the above conclusions are also valid for Λ and Ladder system in both the molecules. We have shown here that AWPI in the UV/VUV and infra-red region can be controlled by choosing different vibrational levels of H_2 and Li_2 molecules. It has been shown elsewhere [23] that AWPI in the visible range can be controlled also by choosing different rotational levels in LiH molecule. In the present work we have studied only the amplification of weak probe field. But the study of the effect of the finite length of the active medium, coupling with cavity modes etc. on the amplification process will be interesting and has been left for future investigation.

In the present work we have set up the density matrix equations by choosing three rovibrational levels of different electronic states. For ladder system we have chosen the ground and two excited electronic states and for V/Λ schemes the ground and the first excited allowed electronic state have been considered. We have solved these equations numerically to obtain time evolution of coherences and populations. We have found that the populations and coherences reach the steady state limit at the asymptotic time i.e. the time which is much greater than the largest characteristic time of the system. To check this we have analytically solved the above equations in the steady state limit i.e. by putting $\dot{\rho}_{ij} = 0$ at the left hand side of all the equations ($3a \rightarrow 3e$) and replacing ($3f$) by the closure relation. It is found that the values of populations and coherences obtained by numerically solving the equations ($3a \rightarrow 3f$) agree with the analytical values obtained by formally solving the equations in the steady state limit. Analytical expressions for the populations and coherences in the steady state limit will be given elsewhere. Simplified analytical expressions for the coherences and the populations can be derived from these formal solutions, under different approximations. But to get the general solutions without approximations [8] and to study the evolution of the system, it is necessary to solve these time dependent equations ($3a \rightarrow 3f$) numerically and to compare these numerical values at the asymptotic time limit with the analytical values obtained from the formal solutions in the steady state limit. From the coherence between two lasing levels we have calculated the gain profile (gain as a function of detuning from the upper lasing level) at different values of evolution time. Numerical values of gain at the asymptotic time have been checked with the analytical values of gain in the steady state limit. We have studied dependence of gain profiles on the choice of transitions involving different vibrational levels with and without Doppler broadening at the room temperature. For all the calculations closure relation for the populations in three levels has been checked.

2 Theory

Figures 1a, 1b and 1c show the schematic diagram for the Ladder, V and Λ transition schemes respectively. The theory for Ladder transition scheme has been given here in detail. The density matrix equations for the V and Λ transition schemes can be derived using similar procedure.

2.1 Ladder transition scheme

We consider a three-level ladder system with ground state $|3\rangle$ and excited states $|2\rangle$ and $|1\rangle$ as illustrated in Figure 1a. The transition $|2\rangle \rightarrow |1\rangle$ of frequency ω_{21} is driven by a strong coupling laser of frequency ω_1. A weak probe laser of frequency ω_2 is applied to the transition $|3\rangle \rightarrow |2\rangle$. An incoherent pump field of rate 2Λ is applied between $|3\rangle$ and $|2\rangle$. $2\gamma_1$ and $2\gamma_2$ are the spontaneous decay rates of the states $|1\rangle$ and $|2\rangle$ respectively. The Rabi frequencies for the coupling and probe fields respectively are given by:

$$\Omega_1 = d_{km}E_1 \tag{1a}$$

$$\Omega_2 = d_{ij}E_2 \tag{1b}$$

where E_1 and E_2 are the electric field for the coupling and probe fields while d_{km} and d_{ij} are the dipole transition moments for the respective transitions. For ladder scheme, $k = 1$, $m = 2$ and $i = 2$, $j = 3$. The detunings between

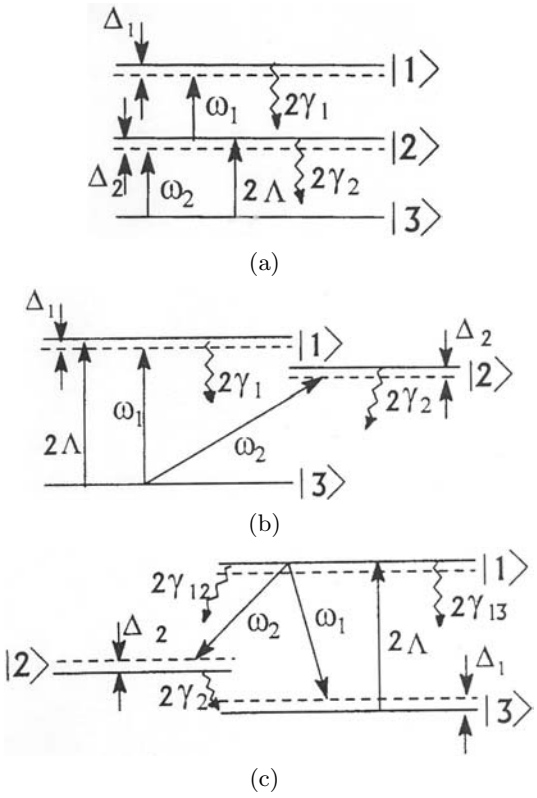

Fig. 1. (a) Schematic diagram for the ladder transition scheme. The probe field of frequency ω_1 and the strong field of frequency ω_2 have been applied between levels $|3\rangle \rightarrow |2\rangle$ and $|2\rangle \rightarrow |1\rangle$ respectively. The level $|2\rangle$ is pumped by the incoherent pumping field of rate 2Λ from level $|3\rangle$. $2\gamma_1$ and $2\gamma_2$ are the spontaneous decay width of levels $|1\rangle$ and $|2\rangle$ respectively. Δ_1 and Δ_2 are the detunings from the levels $|1\rangle$ and $|2\rangle$ respectively. (b) Schematic diagram for three level V scheme. The probe field and the strong field have been applied between levels $|3\rangle \rightarrow |1\rangle$ and $|3\rangle \rightarrow |2\rangle$ respectively. (c) Schematic diagram for three level Λ scheme. Here the strong field has been applied between levels $|1\rangle$ and $|2\rangle$.

the field and the system frequencies are given by:

$$\Delta_1 = \omega_{km} - \omega_1 \tag{2a}$$
$$\Delta_2 = \omega_{ij} - \omega_2. \tag{2b}$$

Under the rotating-wave approximation, the density-matrix equations of motion can be written as:

$$\dot{\rho}_{11} = -2\gamma_1\rho_{11} + i\Omega_1\rho_{21} - i\Omega_1^*\rho_{12} \tag{3a}$$
$$\dot{\rho}_{12} = -(\gamma_1 + \gamma_2 + i\Delta_1)\rho_{12} + i\Omega_1(\rho_{22} - \rho_{11}) - i\Omega_2^*\rho_{13} \tag{3b}$$
$$\dot{\rho}_{13} = -[(\gamma_1 + \Lambda) + i(\Delta_1 + \Delta_2)]\rho_{13} + i\Omega_1\rho_{23} - i\Omega_2\rho_{12} \tag{3c}$$
$$\dot{\rho}_{22} = 2\gamma_1\rho_{11} + 2\Lambda\rho_{33} - 2\gamma_2\rho_{22} + i\Omega_1^*\rho_{12} + i\Omega_2\rho_{32} - i\Omega_1\rho_{21} - i\Omega_2^*\rho_{23} \tag{3d}$$
$$\dot{\rho}_{23} = -[\gamma_2 + \Lambda + i\Delta_2)\rho_{23} + i\Omega_1^*\rho_{13} + i\Omega_2(\rho_{33} - \rho_{22}) \tag{3e}$$
$$\dot{\rho}_{33} = -2\Lambda\rho_{33} + 2\gamma_2\rho_{22} - i\Omega_2\rho_{32} + i\Omega_2^*\rho_{23}. \tag{3f}$$

The above set of equations can be written as a matrix equation,

$$\frac{\partial\rho}{\partial t} = \mathbf{A}\rho \tag{4}$$

which can be solved numerically to obtain the density matrix elements. Here ρ is the density matrix and $\mathbf{A}$ is the coefficient matrix.

The gain coefficient for a three-level system is given as:

$$\mathbf{G} = \frac{-4\pi n\omega_2|d_{ij}|^2}{\hbar c\Omega_2}\mathrm{Im}(\rho_{ij}) \tag{5}$$

where n is the number density of molecules and ρ_{ij} is the coherence term for the transition over which the probe field is applied. For ladder transition scheme, $i = 2$, $j = 3$ in equation (5).

To obtain gain in the steady state, we have formally solved the above equations by putting left hand side equal to zero to obtain analytical values of populations and coherences and hence the gain as a function of detuning.

2.2 V-scheme

In this scheme, the transition $|2\rangle \rightarrow |3\rangle$ is driven by the strong laser while the probe is applied on the transition $|1\rangle \rightarrow |3\rangle$ (Fig. 1b). Rabi frequencies and detunings are given by (1) and (2) with $k = 2$, $m = 3$ and $i = 1$, $j = 3$. The gain coefficient is given by equation (5) with $i = 1$, $j = 3$.

2.3 Lambda scheme

In this three-level scheme, the excited states $|1\rangle$ and $|2\rangle$ are coupled by the strong field, while the upper excited state $|1\rangle$ and the ground state $|3\rangle$ are coupled by a weak probe field (Fig. 1c). Accordingly, the Rabi frequencies and detunings are defined by equations (1) and (2) with $k = 1$, $m = 2$ and $i = 1$, $j = 3$. The gain coefficient is given by equation (5) with $i = 1$, $j = 3$.

To include the effect of Doppler broadening the Doppler widths γ_{D_1} and γ_{D_2} should be added to the decay widths γ_1 and γ_2 respectively for all the three transition schemes. The Doppler widths are defined as:

$$\gamma_{D_i} = 2\omega_i/c\sqrt{2\,(\ln 2)\,kT/m}$$

where ω_i is the frequency for the transition i, m is the reduced mass of the molecule and T is the temperature of the system.

3 Transition schemes

We have considered here three type of transition schemes to study LWPI in H_2 and Li_2 molecules, e.g. Ladder, V and Λ type three level system. In H_2 molecule we have

considered the following transitions:

(i) for ladder system,

$$X^1\Sigma_g{}^+(v,j)\rightarrow B^1\Sigma_u{}^+(v_1,j_1)$$

transitions are coupled by the probe field and

$$B^1\Sigma_u{}^+(v_1,j_1)\rightarrow E,F^1\Sigma_g{}^+(v_2,j_2)$$

transitions are coupled by strong coherent field;

(ii) for V system,

$$X^1\Sigma_g{}^+(v,j)\rightarrow B^1\Sigma_u{}^+(v_1,j_1)$$

transitions are coupled by the probe field and

$$X^1\Sigma_g{}^+(v,j)\rightarrow B^1\Sigma_u{}^+(v_2,j_2)$$

transition is coupled by the strong coherent field;

(iii) for Λ system,

$$B^1\Sigma_u{}^+(v_1,j_1)\rightarrow X^1\Sigma_g{}^+(v,j)$$

transition is coupled by the probe field and

$$B^1\Sigma_u{}^+(v_1,j_1)\rightarrow X^1\Sigma_g{}^+(v_2,j_2)$$

transition is coupled by the strong coherent field.

Similarly for Li_2 molecule we have considered following transitions:

(i) for ladder system,

$$X^1\Sigma_g{}^+(v,j)\rightarrow A^1\Sigma_u{}^+(v_1,j_1)$$

transitions are coupled by the probe field and

$$A^1\Sigma_u{}^+(v_1,j_1)\rightarrow I^1\Pi_g(v_2,j_2)$$

transitions are coupled by the strong coherent field;

(ii) for V system,

$$X^1\Sigma_g{}^+(v,j)\rightarrow A^1\Sigma_u{}^+(v_1,j_1)$$

transitions are coupled by the probe field and

$$X^1\Sigma_g{}^+(v,j)\rightarrow A^1\Sigma_u{}^+(v_2,j_2)$$

transition is coupled by the strong coherent field and vice versa;

(iii) for Λ system,

$$X^1\Sigma_g{}^+(v,j)\rightarrow A^1\Sigma_u{}^+(v_1,j_1)$$

transition is coupled by the probe field and

$$A^1\Sigma_u{}^+(v_1,j_1)\rightarrow X^1\Sigma_g{}^+(v_2,j_2)$$

is coupled by the strong field.

Here v is the vibrational quantum number and j is the angular momentum quantum number for the molecular system. For all the transition schemes incoherent pump field is on the probe transitions.

4 Calculations

For the calculation of gain in H_2 molecules the data for the total dipole transition moments (product of electronic dipole transition moments with the wavefunction of initial and final rovibrational levels and integrated over nuclear coordinates) were taken from the literature [16]. The decay width from different rovibrational levels were calculated from these data. For Li_2 molecules the potential energy curves and the electronic dipole transition moments are available in the literature [22]. We have calculated the total dipole transition moments by integrating the product of electronic dipole transition moments (as a function of internuclear separation) with the wavefunction of initial and final rovibrational levels. Similarly the decay widths from different rovibrational levels were calculated. The coefficient matrix A were constructed from these ab-initio data and diagonalized for different values of detunings from the upper lasing level and evolution time, to calculate the coherences and populations. Calculations have been repeated by considering Doppler Broadening.

5 Results and discussions

We have presented here the results for gain in three level Ladder, V and Λ system as a function of detuning from the upper lasing level in H_2 and Li_2 molecules. Results are given for steady state limit as well as at intermediate values of time to show the evolution of gain profile with time. Since we have chosen a molecular system as a gain medium, it has been shown that the gain profile as well as its magnitude depend on the choice of different rovibrational levels for the probe and strong field transitions. Since the Doppler width at room temperature of these two molecules is orders of magnitude greater than the spontaneous width, we have studied the gain profiles to show the feasibility of amplification under such strong damping. Time evolution of amplification, population inversion and the populations in three levels has been shown considering the Doppler effect.

In H_2 molecule, considering the ladder transition scheme, gain profiles (at the steady state limit) for three different vibrational levels of $B^1\Sigma_u$ state ($v = 0$, 1 and 2 as the upper levels for amplification) have been shown in Figure 2. The strong field coupling for this transition scheme is between these three vibrational levels of $B^1\Sigma_u$ state and $v = 0$ of $E,F^1\Sigma_g$ state. It is found that the AWPI depends on the choice of vibrational levels as the upper level for amplification. This is because of the fact that the dipole transition moment, spontaneous decay and the energy difference of these levels from the lower level are different and the coherence responsible for amplification depends on these system parameters. It is found that the AWPI can be obtained under the condition that the incoherent pumping rate to the upper level is $\leq$ the spontaneous decay rate of that level. Otherwise when Λ is greater than γ (γ_2 for the Ladder scheme and γ_1 for the V and Λ scheme) population get inverted. Since γ's are different for different vibrational levels one has to use

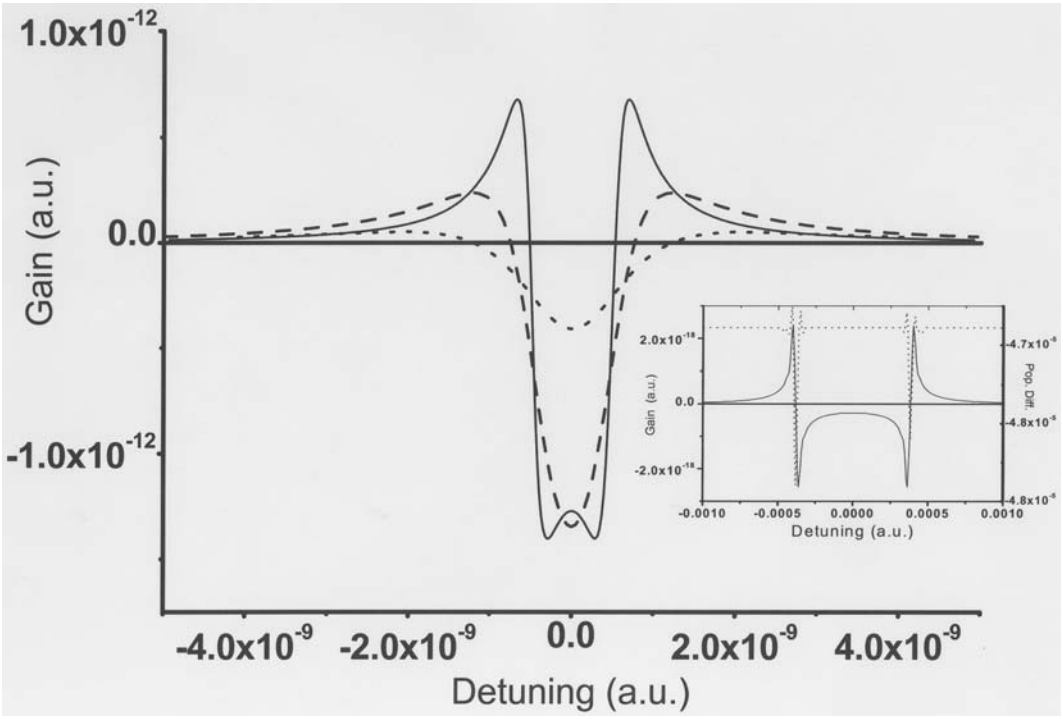

Fig. 2. Ladder scheme in H_2 molecule: gain profile for amplification from three vibrational levels ($v = 0, 1$ and 2) of $B^1\Sigma_u$ state without Doppler broadening. Solid line: $v = 0$, $\gamma_1 = 3.155294\times10^{-11}$ a.u. (0.2077 MHz), $\gamma_2 = 1.108695\times10^{-10}$ a.u. (0.7299 MHz), $\Lambda = 1.1086 \times 10^{-10}$ a.u. (0.7299 MHz); dashed line: $v = 1$, $\gamma_1 = 2.030416 \times 10^{-11}$ a.u. (0.1336 MHz), $\gamma_2 = 3.91735 \times 10^{-10}$ a.u. (2.5792 MHz), $\Lambda = 3.917 \times 10^{-10}$ a.u. (2.5790 MHz) and dotted line: $v = 2$, $\gamma_1 = 7.905192 \times 10^{-12}$ a.u. (0.05204 MHz), $\gamma_2 = 8.039162 \times 10^{-10}$ a.u. (5.2930 MHz), $\Lambda = 8.039 \times 10^{-10}$ a.u. (5.2930 MHz). In the above three calculations $\tau = 10^{12}$ a.u. (2.4188×10^{-5} s), the intensity for probe field $= 9 \times 10^{-6}$ W/cm^2 and the intensity for coherent field $= 10^{-2}$ W/cm^2. For ladder transition the probe field couples level 3 with level 2. For Λ and V scheme probe coupling is between levels 3 and 1 as shown in Figure 1. Inset shows gain profile (solid) and population difference ($\rho_{11} - \rho_{33}$) (dotted) for amplification from $v = 0$ level of $B^1\Sigma_u$ state with Doppler broadening, $\gamma_D = 3.5845 \times 10^{-6}$ a.u. (23.6 GHz). Here almost the same Doppler widths have been considered for labels 1 and 2. $\tau = 10^{10}$ a.u. (2.4188×10^{-7} s), and $\Lambda = 3.5 \times 10^{-6}$ a.u. (23 GHz). Intensity for probe field $= 50$ W/cm^2 and intensity of coherent field $= 6 \times 10^9$ W/cm^2. Here the gain and the detunings are given in a.u. To convert both in the unit of cm^{-1} one will have to divide gain by the factor $0.52917715 \times 10^{-8}$ and to multiply the detuning by the factor 219475.

different Λ to obtain AWPI. In these three sets of calculations the values of strong coherent fields are the same. Similarly the values of the probe fields are chosen to be the same to demonstrate clearly the effect of the choice of different vibrational levels on amplification. Inset shows the gain profile for the transition to the $v = 0$ level of $B^1\Sigma_u$ state at the steady state limit (i.e. at a large time) by considering Doppler broadening. It is found that the gain considering the Doppler broadening is six orders of magnitude less than the gain obtained without considering the Doppler broadening. This is because of the fact that the Doppler width for these transitions are four to six orders of magnitude greater than the spontaneous decay widths. Hence the strength of the coherent field has to be increased by four to six orders of magnitude so that the splitting of two strongly coupled levels exceeds the inhomogeneous broadening. The energy difference between the ground vibrational level ($v = 0, j = 0$) of $X^1\Sigma_g$ state and the $v = 0, 1$ and 2 ($j = 1$) levels of $B^1\Sigma_u$ state are 90125.214 cm^{-1}, 91444.917 cm^{-1} and 92771.643 cm^{-1} respectively. These energy differences correspond to the wavelengths 110.9 nm, 109.3 nm and 107.7 nm respectively. Therefore in H_2 molecule, AWPI can be obtained in the VUV spectral region. Generation of these wavelengths in the laboratory is possible [24] and this can be used as probe field. Regarding the strong field coupling it is found that the intensity required is in the range of $6 \times 10^9 \rightarrow 6 \times 10^{10}$ W/cm^2 (in presence of Doppler broadening). For Ladder-scheme the coherent field wavelengths are 1109.6 nm, 1300 nm and 1560.2 nm for the upper transition from $v = 0, 1$ and 2 levels of $B^1\Sigma_u$ state respectively. Therefore for Ladder configuration AWPI in H_2 molecule is feasible to observe in practice. For the V and Λ schemes the wavelength for coherent transition is 110.9 nm and 114.4 nm respectively. For these wavelengths one can obtain intensity in the abovementioned range by focusing a pulse of energy of nanojoule and duration $\sim$10 ps into the focal area of 10 μm^2. Due to the Doppler broadening, steady states are reached within a short time ($\sim 2\times10^6$ a.u. i.e. $\sim$48 ps), see upper inset in Figure 3. One can also couple these two levels by three-photon transition using lasers of wavelengths in the range of 330 nm and intensity

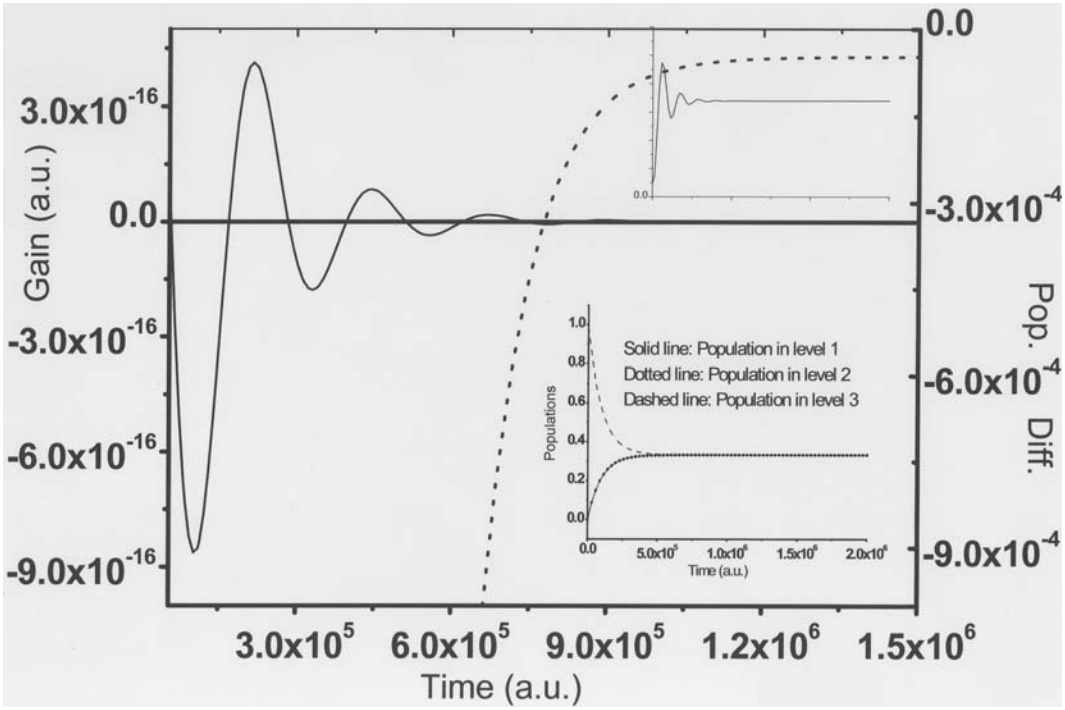

Fig. 3. Gain from $v = 0$ level of $B^1\Sigma_u$ (solid line) and population difference (dotted line) as a function of time with Doppler broadening (for Ladder scheme in H_2 molecule). Detuning from upper lasing level = 4.1×10^{-4} a.u. (89.98 cm^{-1}). For all the results shown in this paper the strong field coupling is considered to be on resonance. The positive gain at large time (steady state limit) is shown in the upper inset. The lower inset shows the evolution of populations in three levels for this transition. Other parameters are the same as in Figure 2. 1 a.u. of time = $2.4188845 \times 10^{-17}$ s.

in the range of 10^{14} W/cm^2. In the calculation of gain ($\sim 10^{-18}$ a.u. i.e. 1.89×10^{-10} cm^{-1}) we have used molecular density of $10^9/cm^3$ but by increasing the molecular density to the value as high as $10^{16}/cm^3$ (pressure less than 1 Torr) one can get gain ($\sim 2 \times 10^{-3}$ cm^{-1}), comparable to He–Ne lasers. For this molecular density the collisional decay width (less than 10 MHz) is much less than the inhomogeneous broadening ($\sim$24 GHz). Rabi frequency for $B^1\Sigma_u(v = 0) \rightarrow E, F^1\Sigma_g(v = 0)$ levels is 2502 GHz which is two orders of magnitude greater than the Doppler width. One can reduce the strong field intensity at the cost of gain but to get appreciable gain AC-Stark splitting should be greater than the Doppler width. It is to be mentioned here that we have plotted the results in a.u., in all the figures. But one can get both the gain and the detunings in the unit of cm^{-1} by dividing the gain by the factor $0.52917715 \times 10^{-8}$ and by multiplying the detunings by the factor 219475 respectively. This is applicable to all the figures showing the gain as a function of detuning. Gain profiles shown here with and without Doppler broadening are the results obtained at the steady state limit. It has been shown [8] previously that the spontaneous decay or the losses towards external states can give rise to damped AWPI. We have also shown here that if the decay widths are increased, as in the case of Doppler broadening the AWPI get damped by orders of magnitude. We have shown here the profiles only with Doppler broadening, since this is the most dominating damping factor for these molecules. From the energy consideration it can be shown that the effect of non-resonant transitions from other states (which get some population due to spontaneous decay from higher states) is negligible. Nevertheless to include the effect of spontaneous decay to other vibrational levels one will have to add the total spontaneous decay width (1.868 GHz, 1.741 GHz and 1.632 GHz for $v = 0$, 1 and 2 of $B^1\Sigma_u$ state respectively) with the Doppler width. Similarly the total spontaneous decay width of $v = 0$ level of $E, F^1\Sigma_g$ should be added to the Doppler width. But since the total spontaneous decay width is at least one order of magnitude smaller than the Doppler width the net effect on the gain profile (with Doppler broadening) will be very small (inset of Fig. 2). Nevertheless it has also been shown [25] before that the population losses can be controlled by repumping.

In Figure 3, evolution of amplification for the emission from $v = 0$ level of $B^1\Sigma_u$ state and the population difference ($\rho_{11} - \rho_{33}$) with time (in a.u.) have been shown to demonstrate that even under large inhomogeneous broadening AWPI is feasible in the VUV range in H_2 molecule. Inset shows the evolution of populations in three levels for the same transitions. It is to be mentioned here that the time in a.u. (plotted in the figures) can be expressed in the unit of seconds multiplying it by the factor $2.4188845 \times 10^{-17}$. This is applicable to all the figures showing the gain, population difference and the populations as a function of time. Evolution of gain has been shown for the detuning at the peak position of the profile (inset) in Figure 2.

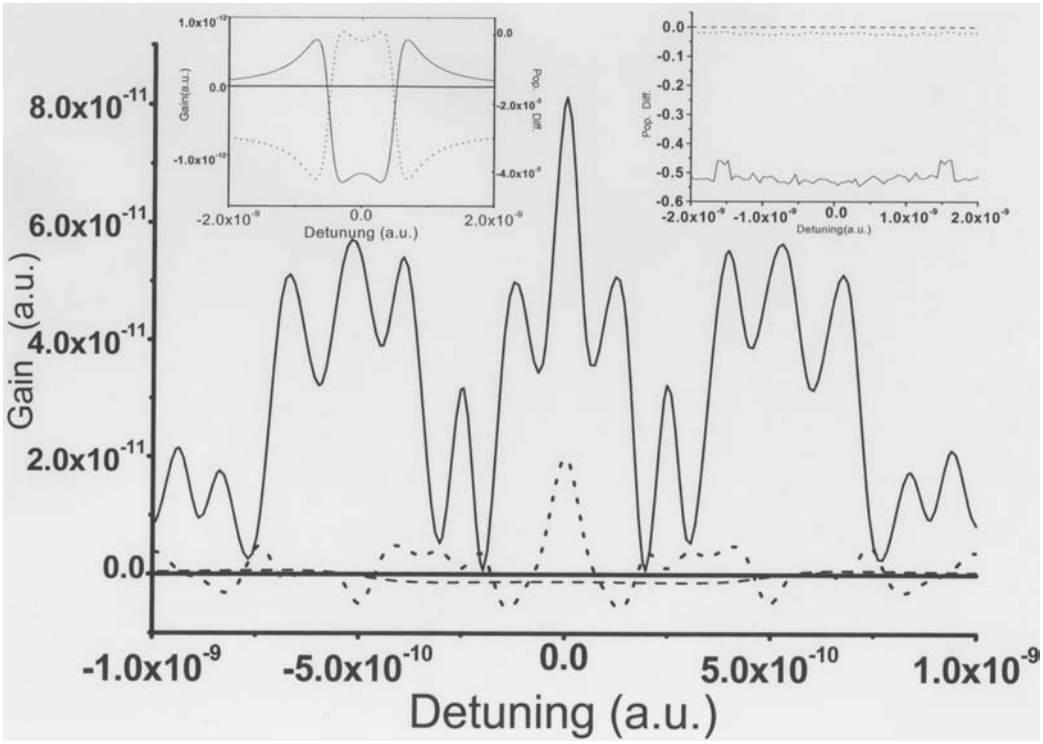

Fig. 4. Transient gain profiles from the $v = 0$ level of $B^1\Sigma_u$ state (Ladder scheme in H_2 molecule) at $\tau = 2 \times 10^9$ a.u. i.e. 4.837×10^{-8} s (solid line), at $\tau = 1.2 \times 10^{10}$ a.u. i.e. 2.578×10^{-7} s (dotted line) and at $\tau = 10^{12}$ a.u. i.e. 2.4189×10^{-5} s (dashed line) (without Doppler broadening) are shown. The right inset shows population differences as function of detuning at the above mentioned times. Solid line at $\tau = 2 \times 10^9$ a.u. (4.837×10^{-8} s), dotted line at $\tau = 1.2 \times 10^{10}$ a.u. (2.902×10^{-7} s) and dashed line at $\tau = 10^{12}$ a.u. (2.4189×10^{-5} s). Other parameters are the same as in Figure 2. Here the dashed line almost coincides with the zero line. Therefore the population difference (dotted line) and the gain profile (solid line) at $\tau = 2.4189 \times 10^{-5}$ s i.e. at the steady state limit, has been shown separately in the left inset.

In Figure 4 we have shown how the gain profile evolves with time for the emission from the $v = 0$ level of $B^1\Sigma_u$ state (in ladder configuration). This shows that the initial amplification at resonance (solid line at $time = 4.8 \times 10^{-8}$ s) get damped with the increase in time at 2.88×10^{-7} s (dotted line) and at large time 2.4×10^{-5} s (dashed line), leading to two peaked gain profile if the Rabi frequency is greater than the decay width. The sponataneous decay time from $v = 0$ levels of $E, F^1\Sigma_g$ and $B^1\Sigma_u$ states are 5 and 1.4 microseconds respectively. Hence for this transition scheme amplification at resonance can be obtained for the time which is less than the sponataneous lifetime of the levels. Under the Doppler free condition in Ladder configuration it has been shown in Li_2 molecule [19] that a single peak in weak-field excitation spectrum splits into two peaks with the increase in the intensity of the strong field. Similar feature can also be obtained in AWPI for the calculations without Doppler broadening (not shown here). Instead of showing the strong field effect on the profile, we have shown here how the single peak profile evolves with time and splits into two peaks in the steady state.

Right inset gives the population difference as a function of detuning at these three evolution times. The gain profile (solid line) and the population difference (dotted line) at the steady state ($time = 2.4 \times 10^{-5}$ s) have been shown separately in the left inset. This shows that at the steady state the gain at resonance is wiped out leading to two peaks symmetrically detuned from the resonance and at these detuned positions population non-inversion is maintained. Hence in the three level Ladder configuration, amplification at resonance can be obtained with pulsed probe (in this case square pulse) of duration 0.3 microsecond or less under Doppler free condition. The gain at a finite time can be obtained if one uses pulsed probe and coherent fields of finite duration (same). One can solve the above density matrix equations at each finite time for different detunings to calculate the coherences and populations at that particular time and hence the gain or amplification by multiplying the imaginary part of the coherence by a constant factor as given in equation (5). In this calculation we have considered constant intensities for the probe and coherent pulses throughout the time of evolution i.e. we have considered square pulses of finite duration. It is to be mentioned here that the spontaneous decay, incoherent pumping and the coherent coupling affect the evolution of coherence differently at each instant of time, depending on the individual time scales. Hence in the case of pulsed probe laser, amplification will depend on the temporal width of the pulses. Temporal evolution of coherences and populations have been studied [1–3, 7, 13] before in different contexts.

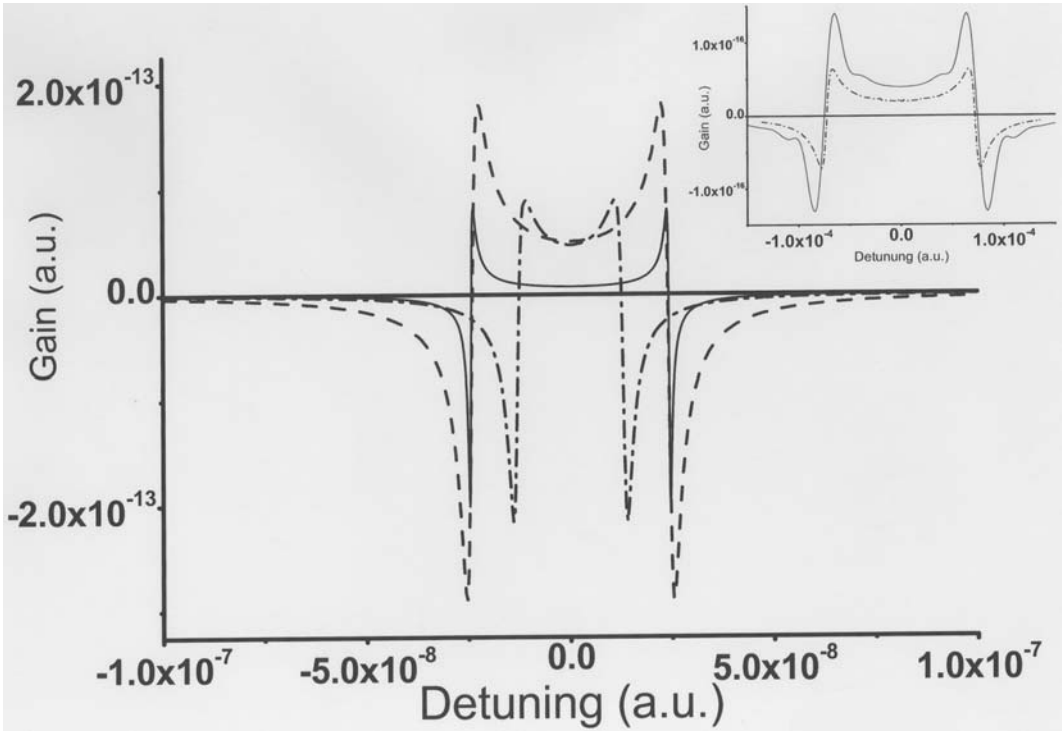

Fig. 5. V-scheme in H_2 molecule: gain profile without Doppler broadening for the transition from $v = 0$ level of $X^1\Sigma_g$ state to the $v = 1$ and 2 levels of $B^1\Sigma_u$ state. Solid line: probe $v = 0 \rightarrow 1$, strong $v = 0 \rightarrow 0$; dashed line: probe $v = 0 \rightarrow 2$, strong $v = 0 \rightarrow 0$ and dot-dashed line: probe $v = 0 \rightarrow 2$, strong $v = 0 \rightarrow 1$. For V-scheme, transitions are between rovibrational levels of $X^1\Sigma_g$ and $B^1\Sigma_u$ states (see text). For the above calculations $\tau = 4 \times 10^{11}$ a.u. (9.675×10^{-6} s), intensity of probe field $= 10^{-5}$ W/cm^2 and intensity of strong field $= 2.0 \times 10^3$ W/cm^2. Other parametrs are the same as in Figure 2. Inset shows gain profiles with Doppler broadening for amplification from $v = 1$ level (solid line) and $v = 2$ level (dashed line) of $B^1\Sigma_u$ state. Strong field couples $v = 0$ levels of $X^1\Sigma_g$ and $B^1\Sigma_u$ states. Probe field intensity $= 1$ W/cm^2, strong field intensity $= 6 \times 10^{10}$ W/cm^2, $\tau = 10^9$ a.u. (2.4188×10^{-8} s) for both the transitions.

Figure 5 shows the dependence of AWPI on vibrational levels ($v = 1$ and 2 levels of $B^1\Sigma_u$ state) chosen as upper levels for amplification in three level V-scheme in H_2 molecule, without Doppler broadening (solid line and dashed line) and with Doppler broadening (inset) at the steady state limit. For these two transition schemes strong coupling has been considered between $v = 0$ levels of $X^1\Sigma_g$ and $B^1\Sigma_u$ states. To demonstrate that the strong field coupling to different vibrational levels can modify the gain profile, we have repeated the calculation with the strong field coupling between $v = 0$ level of $X^1\Sigma_g$ state to the $v = 1$ level of $B^1\Sigma_u$ state, for the probe transition from $v = 0 \rightarrow v_1 = 1$ levels. The effect of different strong field couplings is clear from the two profiles shown in the figure (dashed and dot-dashed lines), without Doppler broadening. The reason for the dependence of AWPI on the choice of vibrational levels for probe and coherent coupling is the same as discussed in the previous paragraph for Ladder transition scheme. As in the case of Ladder transition scheme, it is shown that for three level V-scheme in H_2 molecule AWPI is feasible even in presence of strong Doppler damping (inset) if the intensity of the strong field is made on the order of 10^{10} W/cm^2. Moreover by increasing the density of molecules ($\sim 10^{14}$/ cm^3) one can get amplification of the order of that in He–Ne lasers. By comparing Figures 2 and 5 it is clear that in the steady state limit for V-scheme the maximum gain is orders of magnitude greater than that for ladder scheme and in contrary to Ladder scheme AWPI can be obtained at resonance for V-scheme in H_2 molecule. In section "Theory", we have not given the density matrix equations for V-configurations. But the density matrix equations for the Ladder system shows that replenishment of the ground level due to incoherent pumping has not been considered (i.e. Λ has not been added to the decay widths on the probe transition). In the present case since Λ is less than γ_1 and γ_1 is less than γ_2, replenishment can be neglected and under this condition one can get amplification for V and Λ configurations when both the coherent and probe fields are on resonance. It can also be shown from the analytical analysis (in the steady state limit) that for faster decay on the coherent transition than that on the probe transition, amplification can be obtained under different condition if the replenishment of the ground level is considered. In this calculation we have considered the maximum value of Λ for which maximum gain can be obtained without population inversion. But one can decrease Λ to a lower limit at the cost of magnitude of gain. In absence of incoherent pumping AWPI cannot be obtained [5]. In the inset we have shown the profile with Doppler broadening

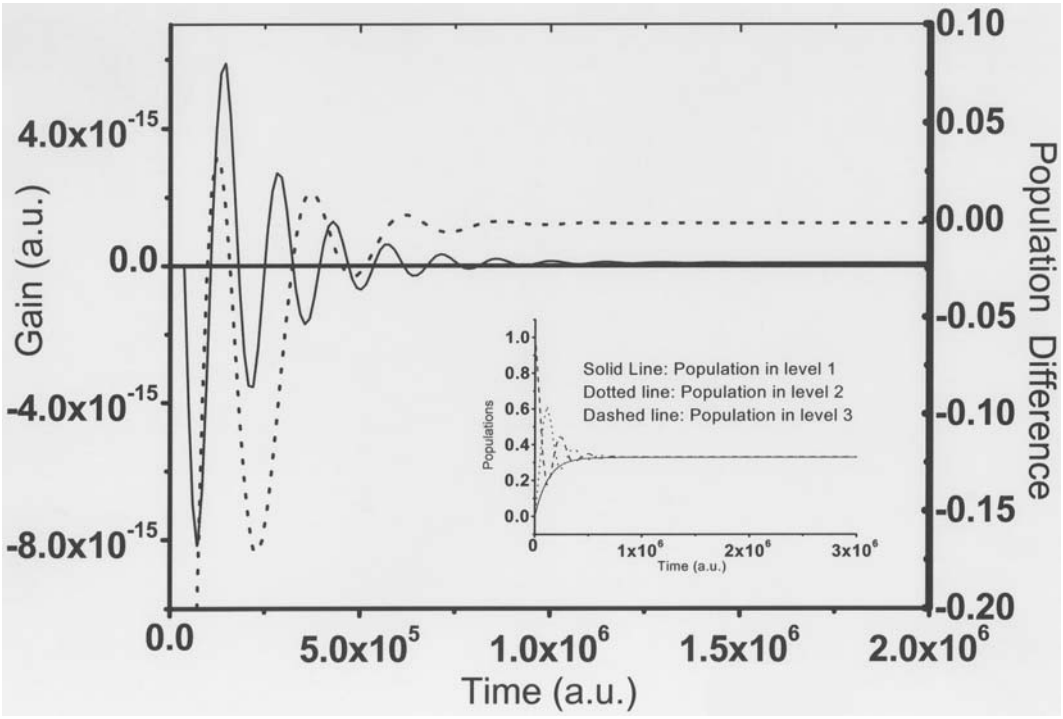

Fig. 6. Evolution of gain (solid line) and population difference (dashed line) with Doppler broadening for probe transition from $v = 0 \rightarrow 2$ and coherent transition from $v = 0 \rightarrow 0$ (V-scheme in H_2 molecule). Detuning from $v = 2$ level is 5.4×10^{-5} a.u. (11.85 cm^{-1}). Inset shows populations in three levels for the above transition. Other parameters are the same as in Figure 5.

for very high strong field intensity so that the peaks are widely separated. Rabi frequency for the strongly coupled levels is 551 GHz. By increasing the strong field intensity from the lower value, step by step, one can show the evolution of splitting of these two peaks [26].

Figure 6 shows the evolution of gain and the population difference (between levels coupled by probe field) with time for the Doppler broadened V-system. The probe transition is between $v = 2$ level of $B^1\Sigma_u$ state and $v = 0$ level of $X^1\Sigma_g$ state and the strong field couples the $v = 0$ levels of $X^1\Sigma_g$ and $B^1\Sigma_u$ states. The inset shows the evolution of population of three levels involved in this transition scheme. From this figure it is clear that amplification persists at large time in absence of population inversion. In V-scheme the population of two strongly coupled states initially oscillates with time to attain the steady state value and this oscillation is imposed on the population difference between two levels coupled by probe field. This shows that the population difference oscillates between inversion and non-inversion at small time before reaching the steady state limit of non-inversion. This feature is different from that for Ladder transition scheme (Fig. 3) where non-inversion is attained throughout the time of evolution, because of the fact that the oscillation of population between two strongly coupled levels is weaker than that in the V-system. In the V-system, the gain with Doppler broadening has been obtained without initial Raman inversion and in the steady state limit $\rho_{11} \leq \rho_{22}$. Since there is no initial Raman inversion one will get only AWPI [8] due to molecular coherences (initial Raman inversion is one of the conditions for superfluorescence).

Figure 7 shows the gain profile for Λ transition scheme in H_2 molecule at the steady state limit, without and with (inset) Doppler broadening. Probe field couples the $v = 0$ level of $X^1\Sigma_g$ state with $v = 1$ level of $B^1\Sigma_u$ state and the strong field coupling is between $v = 1$ levels of $B^1\Sigma_u$ and $X^1\Sigma_g$ states. The wavelength for the strong field transition is 114.4 nm. Inset shows that the maximum gain for Doppler broadened Λ scheme is in between those for V and Ladder schemes in H_2 molecule, when the strong field intensity is of the order of 10^{10} W/cm^2. Similar to V-scheme amplification can be obtained at resonance. The Rabi frequency for the strongly coupled levels is 849.4 GHz. From the results given above it is clear that for the three transition schemes maximum gain can be obtained only around the AC-Stark splitting of the strongly coupled levels, when the splitting is greater than the Doppler width.

Figure 8 shows the evolution of gain and population difference for the same transition scheme considering the inhomogeneous broadening of levels. Inset shows the evolution of population in three levels involved in the transitions. From this figure it is clear that AWPI is possible in three level Λ-system in H_2 molecule in presence of strong Doppler broadening. Although the positive gain in the large time limit is not prominent in the figure (because the initial gain is orders of magnitude greater than the steady state value), the existence of positive gain is confirmed by the profile shown in Figure 7 at the asymptotic

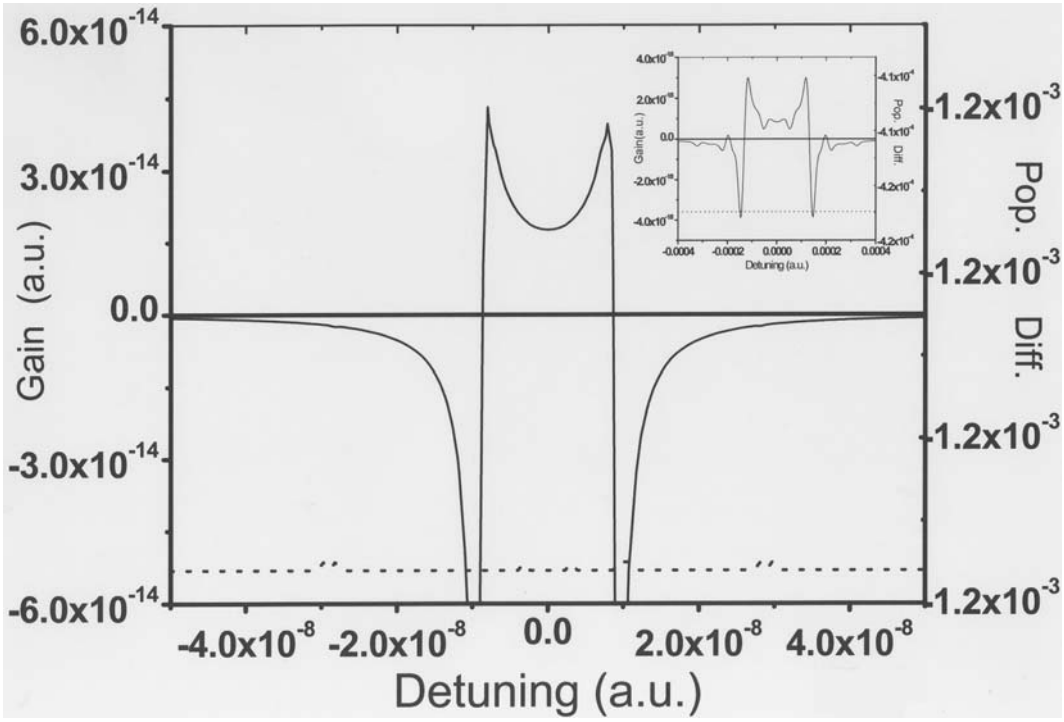

Fig. 7. Λ Scheme in H_2 molecule: gain profile (solid line) and population difference (dotted line) for probe transition $v = 0 \rightarrow 1$ and coherent transition between $v = 1$ levels of $X^1\Sigma_g$ and $B^1\Sigma_u$ states (without Doppler broadening). Probe field intensity $= 10^{-6}$ W/cm^2, strong field intensity $= 50$ W/cm^2 and $\tau = 10^{13}$ a.u. (2.4188×10^{-4} s). Other parameters are the same as in Figure 5. Vibrational relaxation from $v = 1$ level of $X^1\Sigma_g$ state is considered to be one order of magnitude less than that of $v = 1$ level of $B^1\Sigma_u$ state. Inset shows the gain profile (solid line) and population difference (dotted line) with Doppler broadening. Probe field intensity is 1 W/cm^2, Strong field intensity is 10^{10} W/cm^2 and $\tau = 10^{10}$ a.u. (2.4188×10^{-7} s).

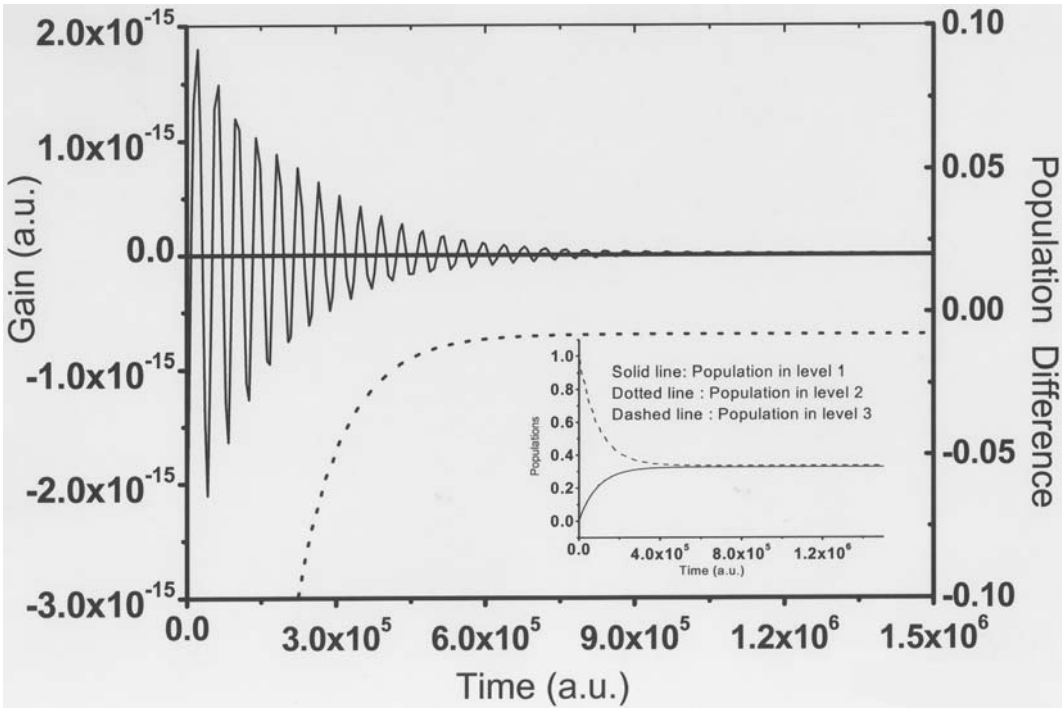

Fig. 8. Evolution of gain (solid line) and population difference (dotted line) with Doppler broadening for the probe transition from $v = 1$ level of $B^1\Sigma_u$ state at the detuning 3.56×10^{-5} a.u. (7.81 cm^{-1}) (Λ scheme in H_2 molecule). Intensities for probe and strong fields are the same as in Figure 7 (inset). Inset shows the corresponding evolution of populations in three levels.

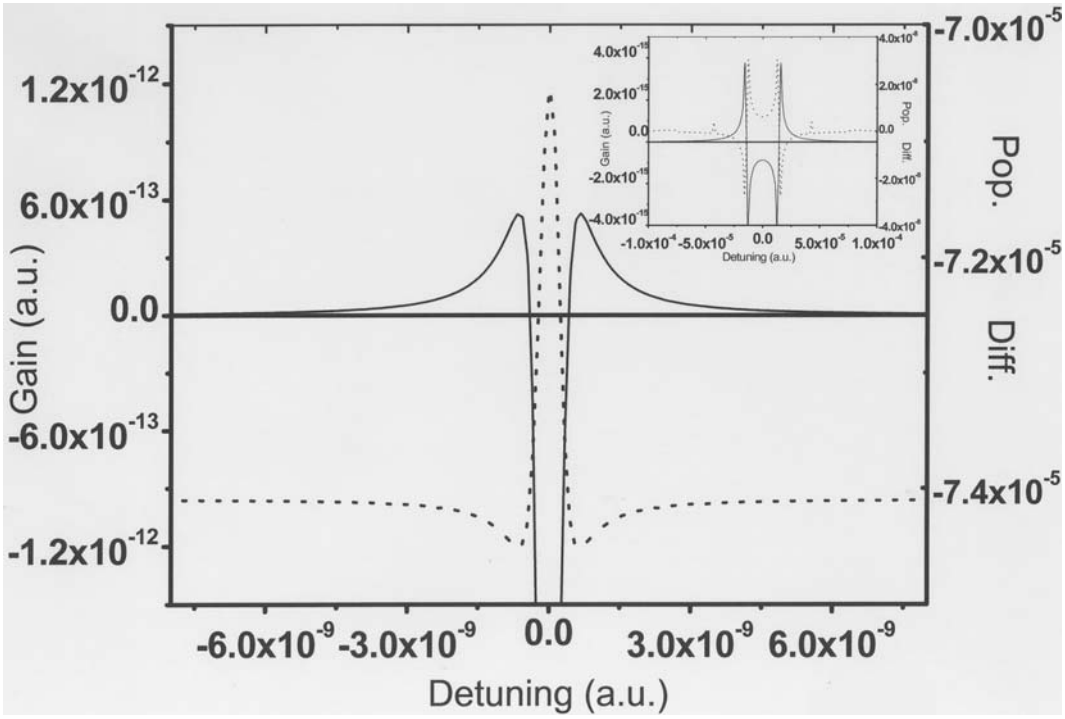

Fig. 9. Ladder scheme in Li_2 molecule: gain profile (solid line) and population difference (dotted line) without Doppler broadening for probe transition between $v = 0$ level of $X^1\Sigma_g$ state and $v = 2$ level of $A^1\Sigma_u$ state and strong coupling between $v = 2$ level of $A^1\Sigma_u$ state and $v = 0$ level of $^1\Pi_g$ state. Probe field intensity is 10^{-5} W/cm^2, strong field intensity is 0.1 W/cm^2 and $\tau = 10^{14}$ a.u. (2.4188×10^{-3} s). $\gamma_1 = 6.974169 \times 10^{-13}$ a.u. (4591.96 Hz), $\gamma_2 = 2.02445 \times 10^{-10}$ a.u. (1.3329 MHz) and $\Lambda = 2.024 \times 10^{-10}$ a.u. (1.33 MHz). Inset shows gain profile (solid line) and population difference (dotted line) with Doppler broadening for the above transition. Doppler width $= 2.1856 \times 10^{-7}$ a.u. (1.439 GHz), $\Lambda = 2.1856 \times 10^{-7}$ a.u. (1.439 GHz), probe field intensity $= 0.1$ W/cm^2, strong field intensity $= 4.0 \times 10^8$ W/cm^2 and $\tau = 10^9$ a.u. (2.4189×10^{-8} s).

time limit. This is true also for the V-transition scheme (see Figs. 5 and 6). Vibrational relaxation width between levels 2 and 1 in V-scheme and between levels 1 and 0 in Λ scheme is orders of magnitude less than the spontaneous decay width.

So far we have discussed about the possibility of AWPI in the H_2 molecule considering three transition schemes (Ladder, V and Λ) and have shown that it is possible to obtain AWPI in the VUV range in spite of large inhomogeneous broadening. We will now show the results for AWPI in Li_2 molecule which can lead to emission in red and infra-red region (photon energies 0.0638418, 0.0649945 and 0.0661289 a.u., and the corresponding wavelengths are 712.9 nm, 700.2 nm and 688.2 nm) for transitions to $v = 0, 1$ and 2 levels of $A^1\Sigma_u$ state respectively from $v = 0$ level of $X^1\Sigma_g$ state. AWPI in visible range has also been described in LiH molecule elsewhere [23]. As in the case of H_2 molecule, we have considered three type of transition schemes (three level Ladder, V and Λ) in Li_2 molecule.

Figure 9 shows the gain profile for three level Ladder transition where the probe field couples $v = 0$ level of $X^1\Sigma_g$ state and $v = 2$ level of $A^1\Sigma_u$ state whereas the coherent coupling is between $v = 2$ level of $A^1\Sigma_u$ state and $v = 0$ level of $^1\Pi_g$ state. The wavelengths for probe and coherent transitions are 688.2 nm and 1379 nm respectively. Inset shows the gain profile for the same transition considering the Doppler broadening of levels at the room temperature. It is found that the population difference (dotted line in the inset) shows two positive peaks only in the region of negative gain. In the region of positive gain population non-inversion is maintained. It is found that the maximum gain considering inhomogeneous broadening is two orders of magnitude less than that obtained without Doppler broadening. For Li_2 molecule Doppler width $\sim 2.1856 \times 10^{-7}$ a.u. (1.439 GHz) is one order of magnitude less than that $\sim 3.5845 \times 10^{-6}$ a.u. (23.6 GHz) of H_2 molecule. Hence the damping due to inhomogeneous broadening is less and the amplification is greater than those in H_2 molecule. As it is expected gain profile with two peaks symmetrically placed in the detuned position around the resonance is obtained. The time evolution of gain and the population inversion for the detuning at the peak position of the profile (inset) in Figure 9 has been shown in Figure 10. The inset shows the evolution of population in three levels involved in the transition.

The gain profile for V-transition scheme in Li_2 molecule is shown in Figure 11 which shows that the profile differs if the probe and the coherent transitions are interchanged. Here probe field couples $v = 0$ level of $X^1\Sigma_g$ state and the $v = 2$ level of $A^1\Sigma_u$ state whereas coherent field couples the $v = 0$ levels of these two electronic states (dot-dashed curve). This profile can be compared with the solid line curve where the two transitions for probe and coherent fields are interchanged. Inset shows

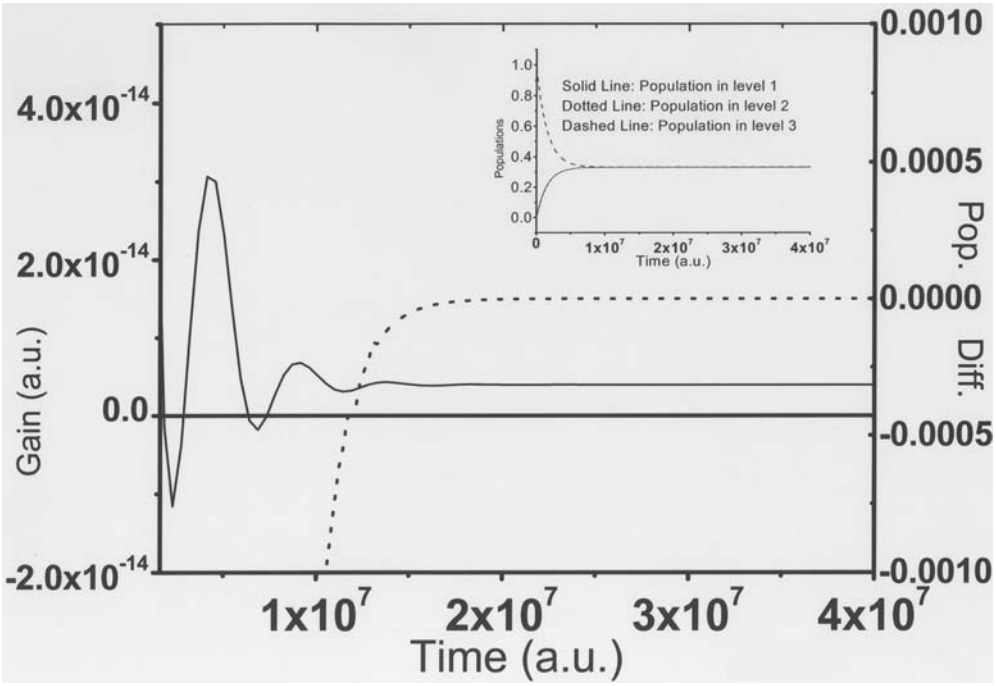

Fig. 10. Evolution of gain (solid line) and population difference (dotted line) with Doppler broadening for the same transition as given in Figure 9 (inset). Detuning = 1.56×10^{-5} a.u. (3.4 cm^{-1}), strong and probe field intensities are the same as given in Figure 9 for Doppler broadened levels. Inset shows evolution of populations in three levels for the above transition.

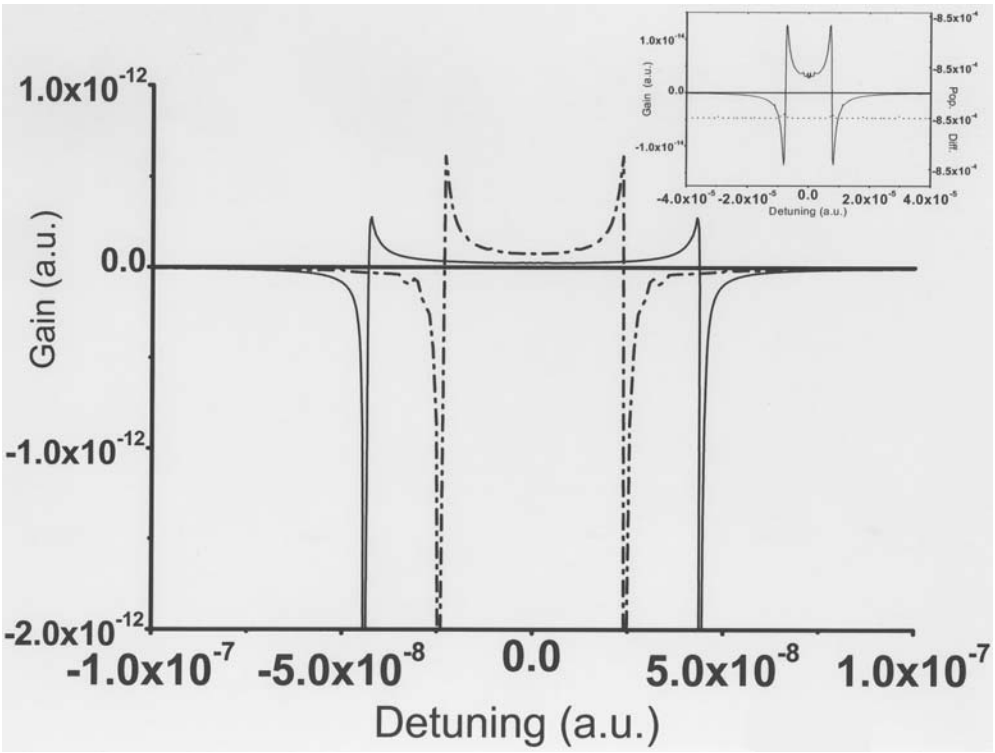

Fig. 11. V-scheme in Li_2 molecule: gain profile without Doppler broadening. Dot-dashed line: probe between $v = 0$ level of $X^1\Sigma_g$ state and $v = 2$ level of $A^1\Sigma_u$ state and strong coupling between $v = 0$ levels of two electronic states mentioned above $\gamma_1 = 2.02445 \times 10^{-10}$ a.u. (1.3329 MHz), $\gamma_2 = 5.47015 \times 10^{-11}$ a.u. (0.3601 MHz) and $\Lambda = 2.02 \times 10^{-10}$ a.u. (1.33 MHz); solid line: probe transition between $v = 0$ levels of two electronic states and coherent coupling between $v = 0$ level of $X^1\Sigma_g$ state and $v = 2$ level of $A^1\Sigma_u$ state. Probe field intensity = 10^{-9} W/cm^2, strong field intensity = 50 W/cm^2 and $\tau = 7 \times 10^{12}$ a.u. (1.69×10^{-4} s) in both the cases. Inset shows gain profile (solid line) and population difference (dotted line) with Doppler broadening. Probe field intensity = 10^{-5} W/cm^2, strong field intensity = 5×10^6 W/cm^2, $\tau = 10^9$ a.u. (2.4188×10^{-8} s) and Doppler width = 2.1856×10^{-7} a.u. (1.439 GHz) and $\Lambda = 2.18 \times 10^{-7}$ a.u. (1.439 GHz).

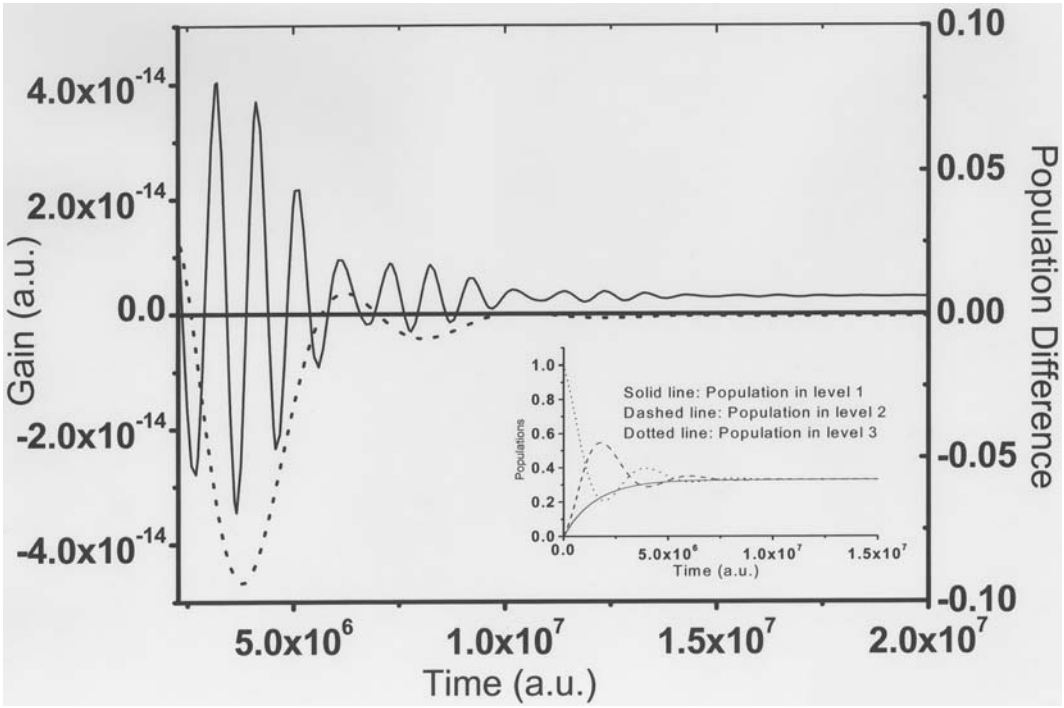

Fig. 12. Evolution of gain (solid line) and population difference (dotted line) with Doppler broadening for the above transition mentioned in Figure 11 (inset). Probe field is also at resonance. Inset shows evolution of populations in three levels for this transition. Probe and strong field intensities are the same as in Figure 11 (inset).

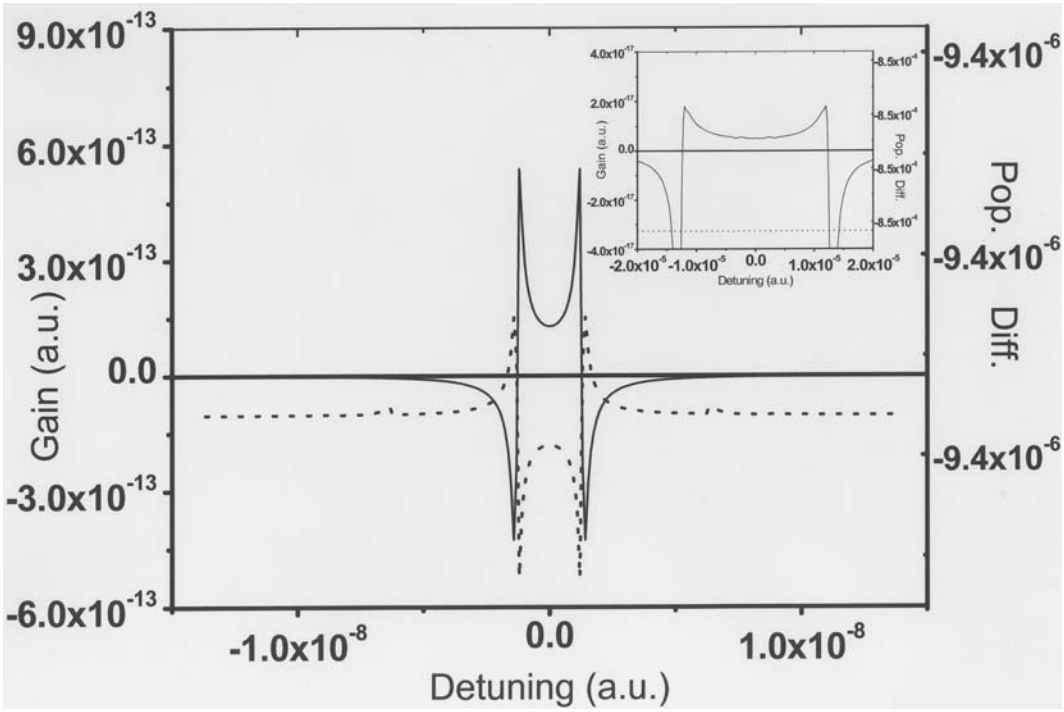

Fig. 13. Λ scheme in Li_2 molecule: gain profile (solid line) and population difference (dotted line) without Doppler broadening for probe transition between $v = 0$ levels of $X^1\Sigma_g$ and $A^1\Sigma_u$ states and coherent coupling between $v = 0$ level of $A^1\Sigma_u$ state and $v = 1$ level of $X^1\Sigma_g$ state. Probe field intensity $= 10^{-6}$ W/cm^2, strong field intensity $= 1.0$ W/cm^2 and $\tau = 10^{13}$ a.u. (2.4188×10^{-4} s). Inset shows gain profile (solid line) and population difference (dotted line) with Doppler broadening for the same transition. Probe field intensity $= 1$ W/cm^2, strong field intensity $= 10^8$ W/cm^2 and $\tau = 10^{10}$ a.u. (2.4188×10^{-7} s).

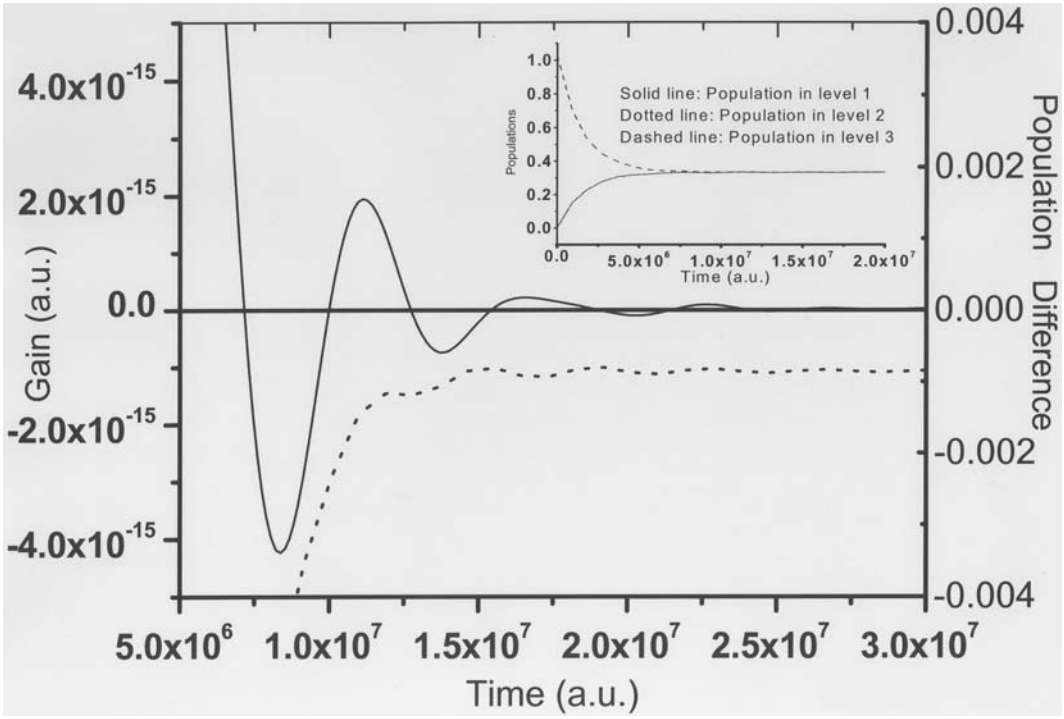

Fig. 14. Evolution of gain (solid line) and population difference (dotted line) with Doppler broadening for the transition mentioned in Figure 13 (inset). Detuning $= 1.18 \times 10^{-5}$ a.u. (2.58 cm^{-1}), probe and the strong field intensities are the same as in Figure 13 (inset). Inset shows evolution of populations in three levels involved in this transition scheme.

the Doppler broadened profile for amplification from $v = 2$ level of $A^1\Sigma_u$ state. Comparison of this profile (inset) with that without considering the inhomogeneous broadening shows that amplification is damped by two orders of magnitude as in the case of Ladder scheme. Time evolution of gain and the population inversion for the detuning at the peak position of the profile with the Doppler broadening is shown in Figure 12. Inset shows the evolution of populations in three levels considered in this transition scheme. It is found that the population in two levels coupled by strong field initially oscillates with time before reaching the steady state value whereas the population of the upper level for amplification increases monotonically with time. This feature of oscillating population is seen in the population difference of two levels coupled by probe but reaches the limit of population non-inversion at large time. Hence it is demonstrated that AWPI can be obtained in Li_2 molecule considering the three level V-scheme. Moreover by increasing the density of molecules one can get amplification of the order of that for He–Ne lasers as discussed in case of H_2 molecule.

In Figure 13, gain profile for Λ transition scheme with (inset) and without inhomogeneous broadening is shown. The probe coupling considered here is between $v = 0$ levels of $X^1\Sigma_g$ and $A^1\Sigma_u$ states and the strong coupling is between $v = 0$ level of $A^1\Sigma_u$ state and $v = 1$ level of $X^1\Sigma_g$ state. The wavelength for coherent transition is 730.9 nm. As in the case of H_2 molecule, maximum gain can be obtained only around the AC-Stark splitting of the strongly coupled levels for the three transition schemes in Li_2 molecule. Therefore one can get an estimate of the Rabi frequency for the coherent transition from the splitting of the gain peaks. From the time evolution of gain, population difference (Fig. 14) and the populations in three levels (inset) at the region of maximum gain (Fig. 13) it is clear that the AWPI is feasible in the steady state limit. At the smaller time the amplification oscillates between positive and negative values whereas the population difference is negative throughout the evolution time. Since the damping due to the inhomogeneous as well as homogeneous broadening in Li_2 molecule is less than that in H_2 molecule, the coherent field intensity required for AWPI in Li_2 is much less ($5 \times 10^6 \rightarrow 4 \times 10^8$ W/cm^2) than that for H_2 molecule. In both the molecules the nature of gain profiles and its magnitude have been shown to differ for three transition schemes. Moreover, the magnitude and the wavelength for amplification are different for these two molecules, in three transition schemes.

In conclusion we have shown here both analytically and numerically that in small diatomic molecules like H_2 and Li_2, AWPI is feasible in the VUV and far-red region respectively both in the case of inhomogeneous and homogeneous broadening of levels. We have also shown that the advantage of choosing molecular system is that the profile of AWPI (as a function of detuning from the upper level of amplification) and the magnitude of maximum gain can be controlled by choosing transitions between different rovibrational levels for three level Ladder, V and Λ transition schemes. We have also shown that the gain profile changes its nature drastically with the time of evolution.

This work has been done under the BRNS project grant No. 2002/37/40/BRNS.

References

1. H. Lee, Y. Rostovtsev, M.O. Scully, Phys. Rev. A **62**, 063804 (2000) and references therein; Y. Zhu, J. Lin, Phys. Rev. A **53**, 1767 (1996); O. Kocharovskaya, Phys. Rep. **219**, 175 (1992); G.S. Agarwal, Phys. Rev. A **55**, 2467 (1997); L.M. Narducci, M.O. Scully, C.H. Keitel, S.Y. Zhu, H.M. Doss, Opt. Comm. **86**, 324 (1991); L.M. Narducci, H.M. Doss, P. Ru, M.O. Scully, S.Y. Zhu, C. Keittel, Opt. Commun. **81**, 379 (1991); see special issue on "Lasing Without Population Inversion", Laser Phys. **9**, No. 4 (1999)
2. S.E. Harris, Phys. Rev. Lett. **62**, 1033 (1989); A. Immamoglu, J.E. Field, S.E. Harris, Phys. Rev. Lett. **66**, 1154 (1991); V.G. Arkhipkin, Yu.I. Heller, Phys. Lett. A **98**, 12 (1983); G.S. Agarwal, S. Ravi, J. Cooper, Phys. Rev. A **41**, 4721 (1990); A. Apalategui, B.S. Mecking, P. Lambropoulos, Laser Phys. **9**, 773 (1999)
3. S. Sanyal, L. Adhya, K. Rai Dastidar, Phys. Rev. A **49**, 5135 (1994); L. Adhya, S. Sanyal, K. Rai Dastidar, Phys. Rev. A **52**, 4078 (1995); Nuovo Cim. D **20**, 1283 (1998); K. Rai Dastidar, L. Adhya, R.K. Das, Pramana **52**, 281 (1999); K. Rai Dastidar, Nature News India, July 1999
4. G. Vemuri, K.V. Vasavada, G.S. Agarwal, Phys. Rev. A **52**, 3228 (1995)
5. J. Gao et al., Opt. Commun. **93**, 323 (1992); A. Nottleman, C. Peters, W. Lange, Phys. Rev. Lett. **70**, 1783 (1993); W.E. Van der Veer et al., Phys. Rev. Lett. **70**, 3243 (1993); J. Kitching, L. Hollberg, Phys. Rev. A **59**, 4685 (1999) and references therein; A.S. Zibrov, M.D. Lukin, D.E. Nikonov, L. Hollberg, M.O. Scully, V.L. Velichansky, H. G. Robinson, Phys. Rev. Lett. **75**, 1499 (1995); E.S. Fry, X. Li, D. Nikonov, G.G. Padmabandhu, M.O. Scully, A.V. Smith, F.K. Tittel, C. Wang, S.R. Wilkinson, Shi-Yao Zhu, Phys. Rev. Lett. **70**, 3235 (1993)
6. Y. Zhu, A.I. Rubiera, Min Xiao, Phys. Rev. A **53**, 1065 (1996); G.S. Agarwal, Phys. Rev. Lett. **67**, 980 (1991)
7. D. Braunstein, R. Shuker, Phys. Rev. A **64**, 053812 (2001) and references therein; D. Braunstein, R. Shuker, Phys. Rev. A **68**, 013812 (2003); G.W. Meyer, U.W. Rathe, M. Graf, Shi-Yao Zhu, E.S. Fry, M.O. Scully, G.H. Harling, L.M. Narducci, Q. Optics: J. Eur. Opt. Soc. B **6**, 231 (1994); L.M. Narducci, M.O. Scully, G.-L. Oppo, P. Ru, J.R. Tredicce, Phys. Rev. A **42**, 1630 (1990)
8. V. Kozlov, O. Kocharovskaya, Y. Rostovtsev, M. Scully, Phys. Rev. A **60**, 1598 (1999); A. Belyanin, C. Bently, F. Cappaso, O. Kocharovskaya, M.O. Scully, Phys. Rev. A **64**, 013814 (2001)
9. A.G. Kafman, G. Kurizki, Opt. Commun. **153**, 251 (1998)
10. Z. Ficek, S. Swain, Uzma Akram, J. Phys. B **34**, 671 (2001); S. Menon, G.S. Agarwal, Phys. Rev. A **61**, 13807 (2000)
11. S. Basile, P. Lambropoulos, Opt. Commun. **78**, 163 (1990); J. Zhang, P. Lambropoulos, X. Tang, Phys. Rev. A **50**, 1935 (1994); D. Petrosyan, P. Lambropoulos, Phys. Rev. A **60**, 398 (1999)
12. D. McGloin, M.H. Dunn, J. Mod. Opt. **47**, 1887 (2000)
13. A.S. Manuka, C.H. Keitel, S.Y. Zhu, M. Fleischhauer, L.M. Narducci, M.O. Scully, Opt. Commun. **94**, 174 (1992)
14. A.V. Popov, S.A. Myslivets, T.F. George, Opt. Exp. **7**, 150 (2000)
15. A. Kuhn, S. Stenerwald, K. Bergmann, Eur. Phys. J. D **1**, 57 (1998)
16. T.E. Sharp, At. Data **2**, 119 (1971); A.C. Allison, A. Dalgarno, At. Data **1**, 289 (1970); M. Glass-Maujean, P. Quadrelli, K. Dressler, At. Data Nucl. Data Tables **30**, 273 (1984)
17. F. Combes, D. Pfenniger, Astron. Astrophys. **327**, 453 (1997) and references therein
18. M. Fleischhaur, C.H. Keitel, M.O. Scully, C. Su, B.T. Ulrich, Shi-Yao Zhu, Phys. Rev. A **46**, 1468 (1992)
19. J. Qi, F.C. Spano, T. Kirova, A. Lazoudis, J. Magnes, L. Li, L.M. Narducci, R.W. Field, A.M. Lyyra, Phys. Rev. Lett. **17**, 173003-I (2002)
20. M.A. Quesada, A.M.F. Lau, D.H. Parker, D.W. Chandler, Phy. Rev. A **36**, 4107 (1987)
21. R.R. Freeman, A.R. Jacobson, D.W. Johusen, N.F. Ramsay, J. Chem. Phys. **63**, 2597 (1975)
22. M.L. Olson, D.D. Konowalow, Chem. Phys. **22**, 29 (1977); Chem. Phys. **21**, 393 (1977); G. Baumgartner, H. Kornmeier, W. Preuss, Chem. Phys. Lett. **107**, 13 (1984); H. Nakatsuji, J. Ushio, Tyonezawa, Can. J. Chem. **63**, 1857 (1985); I. Schmidt-mink, W. Muller, W. Meyer, Chem. Phys. **92**, 263 (1985); D.K. Watson, Chem. Phys. Lett. **51**, 513 (1977); D.D. Konowalow, M.E. Rosenkrantz, D.S. Hochhauser, J. Mol. Spec. **99**, 321 (1983)
23. A. Bhattacharjee, K. Rai Dastidar, J. Mol. Spectrosc. (submitted)
24. H. Rottke, K.H. Welge, Chem. Phys. Lett. **99**, 456 (1983)
25. F. Renzoni, W. Maichen, L. Windholtz, E. Arimondo, Phys. Rev. A **55**, 3710 (1997)
26. J.A. Klienfeld, A.D. Streater, Phys. Rev. A **49**, R4301 (1994)